PROBING THE CGM IN THE NEARBY UNIVERSE IN LYα ABSORPTION: DISCOVERY OF AN GAS ABSORPTION-VELOCITY DICHOTOMY

David M. French, Bart P. Wakker
Department of Astronomy, University of Wisconsin - Madison
Draft version November 20, 2015

ABSTRACT

We present initial results from an ongoing large-scale study of the circumgalactic medium in the nearby Universe ($cz < 10,000 km/s$), using archive Cosmic Origins Spectrograph (COS) sightlines of background QSOs. This initial sample contains 35 sight lines, yielding 154 Lyα systems, 46 of which we have paired with nearby galaxies. We introduce a likelihood parameter to quantitatively predict the galaxy responsible for measured absorption in a reproducible way. We find a dichotomy in the equivalent widths (EW) of absorption systems around $\Delta v = v_{galaxy} - v_{gas}$, with positive Δv absorption EW $= 366 \pm 15$mÅ, and negative Δv absorption EW $= 192 \pm 12$mÅ. We also find a preference for absorption around highly inclined galaxies, but little evidence of azimuthal dependence.

Subject headings: IGM, CGM, galaxies

1. INTRODUCTION

It is well known that galaxies must continue to accrete gas throughout their lifetimes in order to sustain observed levels of star formation (e.g. Erb 2008, Putman et al. 2009b). This additional gas must come from the diffuse intergalactic medium (IGM), where the majority of the baryons in the universe reside (CITATION?). How exactly this IGM gas eventually falls into the halos and disks of galaxies is still highly uncertain, as observational constraints are hard to come by. Because of the diffuse nature of IGM gas, it is most readily and sensitively detected as absorption in the spectra of background active galactic nuclei (AGN). The advent of the sensitive UV spectrographs STIS and COS on the Hubble Space Telescope (HST) have provided a wealth of information on the properties and distribution of both the ions of heavy elements as well as the Lyman series of neutral H I gas around galaxies.

Individual concentrations of gas along a given sightline imprint a 'forest' of absorption lines on the spectrum in the direction of the QSO. The metal lines trace the star formation history within the intervening gas, and neutral hydrogen lines (Lyα) indicate both the location and velocities of outflowing gas as well as the presence of fuel for future star formation. Numerous studies using these observations have shown that Lyα absorbers trace individual galaxy halos (e.g. Wakker & Savage 2009, Danforth et al. 2014, Stocke et al. 2013 & 2014, Liang et al 2014, Lanzetta et al 1995, Chen et al. 1998, 2001a, Tripp et al. 1998, Steidel et al. 2010, Prochaska et al. 2011, Thom et al 2012, Tumlinson et al. 2011 & 2013).

Some recent studies find that about half of Lyα absorbers lie within galaxy haloes, at impact parameters $\rho < 350$ kpc (Côté et al. 2005, Prochaska et al. 2006). In addition, Wakker & Savage (2009) find that for 90% of L> $0.1 L_*$ galaxies an absorber lies within 400 kpc and 400 km/s, and all galaxies have a Lyα absorber within 1.5 Mpc. Higher redshift studies, such as Rudie et al. (2012) at $2 < z < 3$, find evidence for an elevated density of absorbers up to 2 Mpc from galaxies. Wakker & Savage (2009) also confirmed a previously suggested correlation between Lyα absorption linewidth (W) and impact parameter ρ, observing that the broadest lines (FWHM >150 km/s) are only seen within 350 kpc of a galaxy, while at $\rho > 1$ Mpc, only lines with FWHM < 75 km/s occur.

In addition, studying the enrichment of galaxy halos is necessary for constraining outflow models and informing stellar feedback prescriptions. Directly measuring the velocity field and column densities of absorbers as a function of impact parameter and orientation around galaxies would provide the clearest evidence of inflow or outflow activity, but results are still uncertain. Kacprzak et al. (2011) claim to find that Mg II equivalent widths correlate with galaxy inclination, but Mathes et al. (2014) find no such correlation for Lyα and O VI absorbers. Furthermore, we should expect outflowing gas to be more highly enriched and trace the metallicity of the associated galaxy, with inflowing gas instead appearing only in H I. Both Stocke et al. (2013) and Liang & Chen (2014) find an "edge" to heavy ion absorption at $\sim 0.5 R_h$, but with Lyα covering fractions of $\sim 0.75 - 1$ continuing out to R_{vid}. However, Mathes et al. (2014) measures O VI absorption out to $\sim 3 \, D_{gal}/R_{vir}$.

Recent results from Kacprzak et al. (2011 & 2012) suggest that absorbing systems have a preferred orientation with respect to the major and minor axes of the galaxies they are associated with. This could be evidence of inflows and outflows, or an effect of the global structure of galaxy halos, but the statistics are not yet good enough to provide consistent answers. A larger-scale study of inclination and azimuthal angles vs. absorber properties for the largest galaxies in the nearby universe, where it is possible to obtain inclinations and unambiguous absorber associations, is needed in order to elucidate the distribution of absorbing systems around galaxies.

These previous studies have suffered from small sample sizes (e.g. Mathes et al. 2014 use 14 galaxies, Stocke et al. 2013 use 11, Werk et al. 2014 use 44), and incompleteness due to their higher mean redshifts (e.g. the Mathes et al. 2014 sample is $0.12 < z < 0.67$, and Werk et al. 2014 are complete to $\sim L^*$ at $z \sim 0.2$). To address these shortcomings, we are conducting a large sur-

vey of the properties of intergalactic gas in the nearby universe, where we have good and relatively complete information on both faint and bright galaxies, in order to reveal how the IGM and galaxies affect each other. We are taking advantage of the over 300 archived QSO and Seyfert spectra taken by the Cosmic Origins Spectrograph (COS) on the Hubble Space Telescope (HST), combined with the wealth of information available for the $\sim 100,000$ galaxies with $cz < 10,000$ km/s found in the NASA Extragalactic Database (NED) to probe the environment of absorbing gas systems in the nearby universe. This approach allows for an unbiased understanding of the distribution of the gas around galaxies, which requires looking for both detections and non-detections of gas, both near as well as far away from galaxies.

This paper presents initial results from our pilot study of 35 COS sight lines, chosen for their proximity to large galaxies and ease of spectral feature identification. This paper is organized as follows: in Section 2 we present the data and analysis techniques, in Section 3 we present the results, and in Section 4 we discuss possible interpretations of our results.

2. DATA AND ANALYSIS

This initial pilot study contains 35 sightlines to bright QSOs observed with the Cosmic Origins Spectrograph (COS). We chose sight lines based on high S/N (generally >10), ease of spectral identification, and proximity to large, nearby galaxies. Several are included simply because they already have published identifications. There were no strict cutoffs for galaxy size or brightness, we simply selected the top 35 sight lines after rejecting those with lower S/N and/or more complicated features. Table 1 summarizes the properties of the QSO targets we selected. **Should this just be a single table with all absorption features, associated galaxies and QSO info combined?**

All COS spectra for the target sight lines was obtained through the Barbara A. Mikulski Archive for Space Telescopes (MAST), and processed with the latest available version of the CALCOS pipeline **WHICH IS??**. We combined individual exposures by the method of Wakker et al. (2015, submitted), which corrects the COS wavelength scale by cross-correlating all ISM and IGM lines in each exposure. This method addresses the up to ±40 km/s misalignments produced by CALCOS, and produces a corrected error array based on Poisson noise, which better matches the measured errors. We then combine multiple exposure by aligning Galactic absorption lines with 21-cm spectra, and adding up the total counts in each pixel before converting to flux using the original, average flux-count ratio at each wavelength. Spectral features were both identified by eye and by a custom identification algorithm **MORE ABOUT THIS**. Only features identified with high probability by both methods are included in this dataset.

2.1. Galaxy Data

Each final, combined, and identified sightline is correlated with the galaxy environment in order to match absorption features with galaxies near the sightline. To facilitate this, we have constructed a dataset of all $z \leq 0.033$ ($v \leq 10,000$km/s) galaxies with published data available through the NASA Extragalactic

AGN name	z	S/N
MRK290	0.0296	32
SBS1537+577	0.0734	12
3C66A	0.444	24
MRC2251-178	0.0661	29
SBS1503+570	0.3589	11
SDSSJ080838.80+051440.0	0.361	8
2dFGRS_S393Z082	ERR	ERR
PG1211+143	0.0804	19
TON488	0.2564	7
SDSSJ135341.03+361948.0	0.147	11
MRK1014	0.163	14
RX_J1503.2+6810	0.114	8
PG1302-102	0.2784	6
SBS1108+560	0.765	17
PG1216+069	0.3313	24
IRAS_Z06229-6434	0.1289	18
SDSSJ080908.13+461925.6	0.6563	9
TON1009	0.809	10
RX_J1330.8+3119	0.241	11
SDSSJ140428.30+335342.0	0.549	8
RX_J0714.5+7408	0.371	17
PG1121+423	0.234	24
RBS2070	0.165	25
3C351.0	0.3719	ERR
HE1228+0131	0.117	69
3C273.0	0.1583	97
PG1626+554	0.133	20
PG1307+085	0.155	23
PKS2005-489	0.071	32
CSO395	0.169	10
HS0624+6907	0.37	8
HE0238-1904	0.631	36
RBS1795	0.344	35
H1101-232	0.186	16
1H0717+714	0.5003	40
PG0003+158	0.4509	29
SBS1122+594	0.858	10

Table 1
Names, redshifts, and S/N of AGN targets.

Database (NED[1]). This dataset contains over 108,000 entries, and includes data from SDSS, 2MASS, 2dF, 6dF, RC3, and many other, smaller surveys. Our criteria for including a galaxy in this dataset is only an accurate, spectroscopic redshift which places the galaxy in the $400 \leq v \leq 10,000$km/s velocity range. This restriction naturally leads to a completeness limit of $B \lesssim 18.7$ mag **CHECK THIS**, or $\sim 0.1L_*$ on average across the sky (see Figure 1). For any particular region of the sky, this limit will vary some depending upon which of the larger surveys cover the region.

In addition, we have homogenized the galaxy data beyond the steps taken by NED by normalizing all measurements of galaxy inclination, position angle, and diameter to 2MASS K-band values. 2MASS values were chosen for this because it was an all-sky survey, and represents the largest fraction of available galaxy data. Physical galaxy diameters are derived from 2MASS K_s "total" angular diameter measurements and galaxy distances. 2MASS K_s "total" diameter estimates are surface brightness extrapolation measurements and are derived as
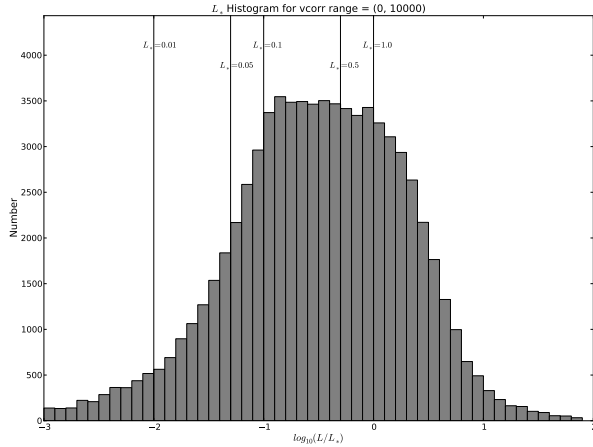
Figure 1. Distribution of L/L_* values for all galaxies in the dataset. Black vertical lines highlight 1, 0.5, 0.1, 0.05 and 0.01 L_*. The turnoff around $0.1L_*$ shows that on average, the dataset is complete to $0.1L_*$.

$$r_{tot} = r' + a(ln(148))^b, \qquad (1)$$

where r_{tot} is defined as the point where the surface brightness extends to 5 disk scale lengths, r' is the starting point radius ($> 5" - 10"$ beyond the nucleus, or core influence), and a and b are Sersic exponential function scale length parameters ($f = f_0 \exp(-r/a)^{(1/b)}$, see Jarret et al. 2003 for a full description). **NEEDS TO BE CHECK FOR FULL SKY** Approximately 50% of all the galaxies have this 2MASS K_s "total" diameter. Of the remainder, 20% have SDSS diameters, 27% have no published diameter, and 3% have diameters from other surveys. We convert these other estimates to 2MASS K_s "total" diameters via a simple least squares linear fit.

We used B-band magnitudes to estimate each galaxy's luminosity as a ratio of L_* as follows:

$$\frac{L}{L_*} = 10^{-0.4(M_B - M_{B_*})}. \qquad (2)$$

We adopt the CfA galaxy luminosity function by Marzke et al. (1994), which sets $B_* = $ -19.57. Direct B band measurements are available for $\sim$ 30% of galaxies, and most of the rest have SDSS g and r magnitudes, which can be converted to B via $B = g + 0.39(g-r) + 0.21$ (Jester et al. 2005). Finally, we also compute an estimate of the virial radius of each galaxy as $logR_{vir} = 0.69logD + 1.24$. This follows the parametrization of Stocke et al. (2013) relating a galaxy's luminosity to its virial radius, and the Wakker & Savage (2009) empirical relation between diameter and luminosity (see Wakker et al. 2015 and references therein for further details).

This homogeneous galaxy data table allows us to draw direct comparisons between the properties of the absorbers and the properties, separations, and environments of nearby galaxies, with unprecedented completeness.

3. RESULTS

We have identified 154 Lyα absorption lines in the spectra of 35 background QSOs. Of these, 32% can be unambiguously associated with a single nearby galaxy,
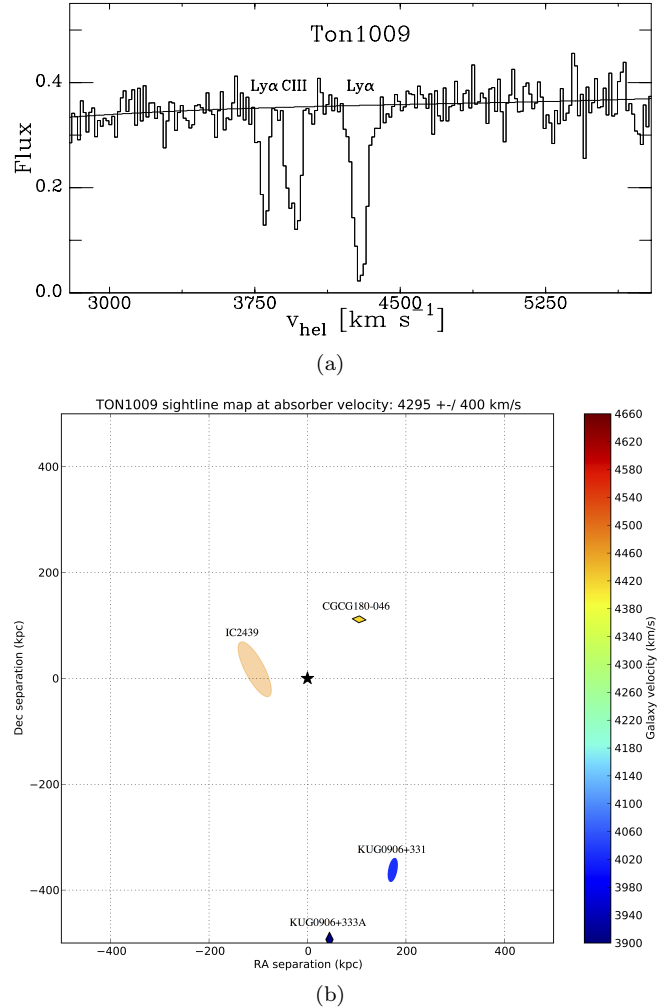

(a)

(b)

Figure 2. a) An example Lyα line found in a sightline towards target TON1009 at 4295 km/s. b) A map of *all* galaxies within a 500 kpc impact parameter target TON1009 sightline and with velocity (cz) within 400 km/s of absorption detected at 4295 km/s (central black star). The galaxy IC2439 (v = 4494 km/s, inclination = 71°) can be unambiguously paired with the Lyα absorption feature at v = 4295 km/s because it is the largest and closest galaxy in both physical and velocity space to the absorption feature.

while 51% reside in relative voids. In order to be considered for a pairing, a galaxy and absorption feature must appear within 400 km/s in velocity and 500 kpc in physical impact parameter from each other. When multiple galaxies pass these criteria for a particular line, we are left with two options. 1) one galaxy is obviously far larger and closer in physical and velocity space to the line, and may have several satellite galaxies, or 2) no single galaxy if obviously dominant, and we do not include this line in further analysis.

To facilitate this decision, we compute the likelihood, $\mathcal{L}$, of every possible galaxy-absorber pairing as follows:

$$\mathcal{L} = Ae^{-(\frac{\rho}{R_{vir}})^2}e^{-(\frac{\Delta v}{200})^2}. \qquad (3)$$

Here ρ is the physical impact parameter, R_{vir} the virial radius of the galaxy, Δv the velocity difference between the absorber and the galaxy ($\Delta v = v_{galaxy} - v_{absorber}$),

and A is a factor included to increase the likelihood in the case that $R_{vir} \geq \rho$ (in which case $A = 2$, otherwise $A = 1$). An absorber-galaxy system separated by 200 km/s in velocity and $1R_{vir}$ would have $\mathcal{L} = 0.27$. In order for an absorber to be marked as "associated" with a particular galaxy, its $\mathcal{L}$ must be a factor of 5 larger than the next best possible association.

Figures 2.1 and 2(b) show a clean example of a Lyα absorption line with a map of its galaxy environment, showing an unambiguous pairing between the absorption feature at $4295km/s$ toward TON1009 and galaxy IC2439 ($\mathcal{L} = 0.45$). Unless explicitly stated, all following analysis concerns similarly unambiguous "associated" systems.

3.1. *W-ρ Anti-correlation*

As mentioned earlier, numerous previous studies have found that Lyα equivalent width (EW) is anti-correlated with impact parameter (ρ) to the nearest galaxy. We find this to be true only when normalizing impact parameters by the galaxy diameter. Figure 3.1 shows a straight comparison between Lyα EW and ρ, where no correlation either way is apparent. Figure 3.1 shows that the expected anti-correlation clearly emerges when plotting EW vs $\rho/diameter$. The obvious explanation for this is that larger galaxies host larger, more physically extent CGM halos. **NEED TO PLOT** ρ/R_{VIR} **INSTEAD**

Most interestingly, new results emerge when we split the absorber-galaxy catalog based on the velocity difference of the two. We define the differential velocity between the absorption and an associated galaxy as follows:

$$\Delta v = v_{galaxy} - v_{absorber}. \qquad (4)$$

With this scheme, we refer to an absorber with a velocity *lower* than the associated galaxy as *blueshifted*, while an absorber with a velocity *higher* is referred to as *redshifted*. The rest of the results will be analyzed based upon this splitting. For all distributions, we employ and quote the results of both the Kolmogorov-Smirnov (KS) and the Anderson-Darling (AD) statistical tests.

3.2. *Inclination*

In this section we examine the inclinations of the associated galaxies compared to the red and blueshifted distributions of absorbers. Figure 4 shows red and blueshifted absorbers' EW plotted against the inclinations of their associated galaxies. We note that there is a clear dichotomy between the distributions, where blue shifted absorbers appear around nearly all inclinations of galaxies, but redshifted absorbers only appear near highly-inclined galaxies (i.e. inclination > 50 deg). In addition, redshifted absorbers appear with lower W than those blueshifted across all inclinations. The average equivalent width of all redshifted absorbers is $\langle W \rangle$ = 192 ± 12mÅ, compared to $\langle W \rangle$ = 366 ± 15mÅ for blueshifted absorbers. We can reject the null hypothesis that red and blue shifted absorbers come from the same underlying distribution at the 95% level (results of both KS and AD tests).

3.3. *Azimuth*

In this section we examine properties of absorbers as a function of their azimuthal angle with respect to their
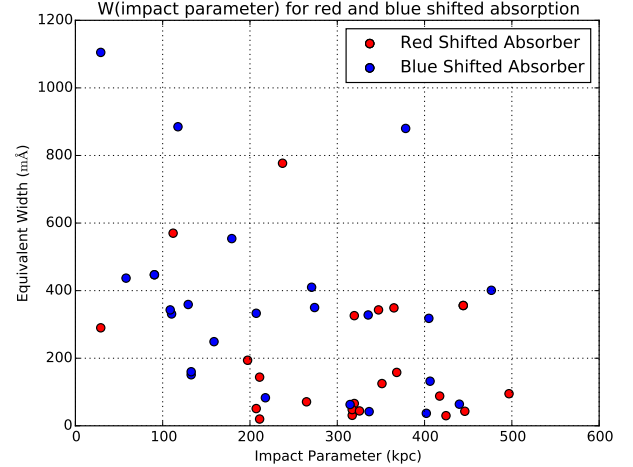
(a)
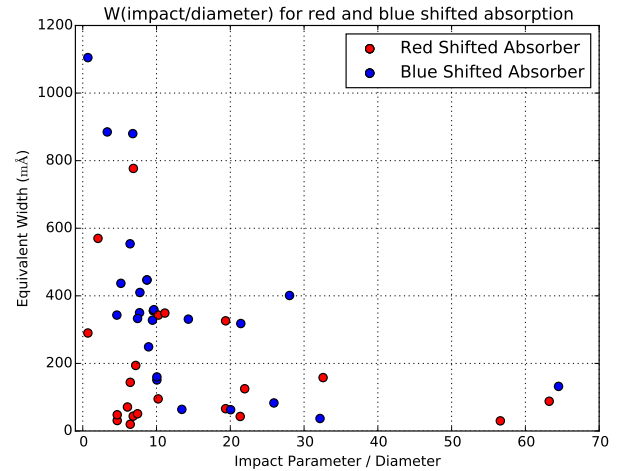
(b)

Figure 3. a) Equivalent width (W) of each absorber as a function of ρ (kpc), the physical impact parameter between the galaxy and the sightline toward the absorption feature. b) (W) as a function of ρ/D, the ratio of the physical impact parameter and the galaxy diameter. A strong anti-correlation is evident only when scaling ρ by the galaxy diameter.

associated galaxy. Azimuth is defined as the angle between the major axis of a galaxy and the vector connecting the absorption feature and the midpoint of the galaxy plane. Figure **??** illustrates this. The mean azimuth angle for all absorption systems is **MEAN AZIMUTH ANGLE**. Again splitting the results into blue and redshifted bins leads to a slight separation in azimuth. We find a mean azimuth angle of **BLUESHIFTED AZIMUTH** for blue shifted absorbers, and **RED SHIFTED AZIMUTH** for redshifted absorbers.

We detect no significant difference between the diameter of the galaxies associated with red vs blue shifted absorbers.

4. DISCUSSION

WHAT'S THE MEAN L_* OF ASSOCIATED GALAXIES? AND ALL THE FIELDS IN GENERAL?
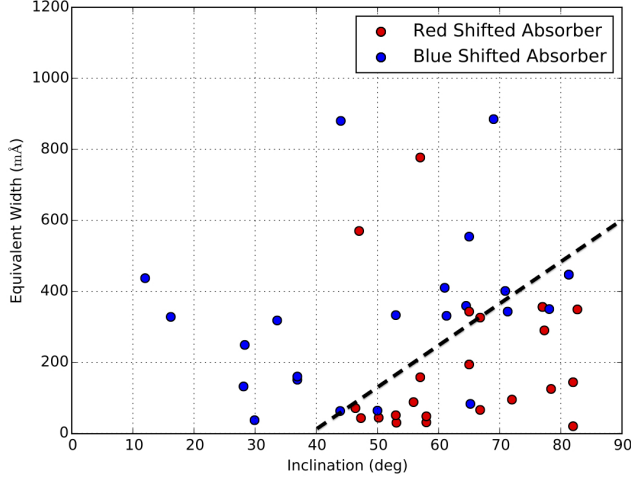
Figure 4. Equivalent width (W) of each absorber as a function of the inclination angle of the associated galaxy in the pilot study sample. The dashed black line is drawn to highlight the separation between red and blue shifted absorption systems (with respect to the systemic velocity of the galaxy).

REFERENCES

Carswell, B., Schaye, J., & Kim, T.-S. 2002, ApJ, 578, 43
Cen, R. 2013, ApJ, 770, 139
—. 2014, ApJ, 789, L21
Chen, H.-W., Lanzetta, K. M., Webb, J. K., & Barcons, X. 1998, ApJ, 498, 77
—. 2001, ApJ, 559, 654
Corwin, Jr., H. G., Buta, R. J., & de Vaucouleurs, G. 1994, AJ, 108, 2128
Côté, S., Wyse, R. F. G., Carignan, C., Freeman, K. C., & Broadhurst, T. 2005, ApJ, 618, 178
Danforth, C. W., & Shull, J. M. 2005, ApJ, 624, 555
—. 2008, ApJ, 679, 194
Danforth, C. W., Shull, J. M., Rosenberg, J. L., & Stocke, J. T. 2006, ApJ, 640, 716
Erb, D. K. 2008, ApJ, 674, 151
Kacprzak, G. G., Churchill, C. W., Barton, E. J., & Cooke, J. 2011a, ApJ, 733, 105
Kacprzak, G. G., Churchill, C. W., Evans, J. L., Murphy, M. T., & Steidel, C. C. 2011b, MNRAS, 416, 3118
Kacprzak, G. G., Churchill, C. W., & Nielsen, N. M. 2012, ApJ, 760, L7
Keeney, B. A., Stocke, J. T., Syphers, D., et al. 2013, in American Astronomical Society Meeting Abstracts, Vol. 222, American Astronomical Society Meeting Abstracts, 214.18
Kereš, D., & Hernquist, L. 2009, ApJ, 700, L1
Kim, T.-S., Bolton, J. S., Viel, M., Haehnelt, M. G., & Carswell, R. F. 2007, MNRAS, 382, 1657
Lanzetta, K. M., Bowen, D. V., Tytler, D., & Webb, J. K. 1995, ApJ, 442, 538
Liang, C. J., & Chen, H.-W. 2014, MNRAS, 445, 2061
Lundgren, B. F., Brunner, R. J., York, D. G., et al. 2009, ApJ, 698, 819

Mathes, N. L., Churchill, C. W., Kacprzak, G. G., et al. 2014, ApJ, 792, 128
McLin, K. M., Stocke, J. T., Weymann, R. J., Penton, S. V., & Shull, J. M. 2002, ApJ, 574, L115
Meiksin, A. A. 2009, Reviews of Modern Physics, 81, 1405
Oppenheimer, B. D., & Davé, R. 2009, MNRAS, 395, 1875
Oppenheimer, B. D., Davé, R., Katz, N., Kollmeier, J. A., & Weinberg, D. H. 2012, MNRAS, 420, 829
Prochaska, J. X., Weiner, B., Chen, H.-W., Mulchaey, J., & Cooksey, K. 2011, ApJ, 740, 91
Prochaska, J. X., Weiner, B. J., Chen, H.-W., & Mulchaey, J. S. 2006, ApJ, 643, 680
Putman, M. E., Peek, J. E. G., & Heitsch, F. 2009a, ArXiv e-prints
Putman, M. E., Henning, P., Bolatto, A., et al. 2009b, in Astronomy, Vol. 2010, astro2010: The Astronomy and Astrophysics Decadal Survey, 241
Rudie, G. C., Steidel, C. C., & Pettini, M. 2012a, ApJ, 757, L30
Rudie, G. C., Steidel, C. C., Shapley, A. E., & Pettini, M. 2013, ApJ, 769, 146
Rudie, G. C., Steidel, C. C., Trainor, R. F., et al. 2012b, ApJ, 750, 67
Shull, J. M., Smith, B. D., & Danforth, C. W. 2012, ApJ, 759, 23
Smith, B. D., Hallman, E. J., Shull, J. M., & O'Shea, B. W. 2011, ApJ, 731, 6
Steidel, C. C., Erb, D. K., Shapley, A. E., et al. 2010, ApJ, 717, 289
Stewart, K. R., Kaufmann, T., Bullock, J. S., et al. 2011, ApJ, 738, 39
Stocke, J. T., Keeney, B. A., Danforth, C. W., et al. 2013, ApJ, 763, 148
Tejos, N., Morris, S. L., Crighton, N. H. M., et al. 2012, MNRAS, 425, 245
Tejos, N., Morris, S. L., Finn, C. W., et al. 2014, MNRAS, 437, 2017
Thom, C., Tumlinson, J., Werk, J. K., et al. 2012, ApJ, 758, L41
Tripp, T. M., Aracil, B., Bowen, D. V., & Jenkins, E. B. 2006a, ApJ, 643, L77
Tripp, T. M., Bowen, D. V., Sembach, K. R., et al. 2006b, in Astronomical Society of the Pacific Conference Series, Vol. 348, Astrophysics in the Far Ultraviolet: Five Years of Discovery with FUSE, ed. G. Sonneborn, H. W. Moos, & B.-G. Andersson, 341
Tripp, T. M., Lu, L., & Savage, B. D. 1998, ApJ, 508, 200
Tripp, T. M., Sembach, K. R., Bowen, D. V., et al. 2008, ApJS, 177, 39
Tully, R. B., Courtois, H. M., Dolphin, A. E., et al. 2013, AJ, 146, 86
Tumlinson, J., Werk, J. K., Thom, C., et al. 2011, ApJ, 733, 111
van de Voort, F., & Schaye, J. 2012, MNRAS, 423, 2991
van de Voort, F., Schaye, J., Booth, C. M., Haas, M. R., & Dalla Vecchia, C. 2011, MNRAS, 414, 2458
Wakker, B. P., Hernandez, A. K., French, D., et al. 2015, ArXiv e-prints
Wakker, B. P., & Savage, B. D. 2009, ApJS, 182, 378
Werk, J. K., Prochaska, J. X., Tumlinson, J., et al. 2014, ApJ, 792, 8
York, D. G., vanden Berk, D., Richards, G. T., et al. 2005, in IAU Colloq. 199: Probing Galaxies through Quasar Absorption Lines, ed. P. Williams, C.-G. Shu, & B. Menard, 58–64